JOURNAL OF Materials CHEMISTRY

Magnetic properties of Co–Al, Ni–Al, and Mg–Al hydrotalcites and the oxides formed upon their thermal decomposition

Javier Pérez-Ramírez,†*[a] Antonio Ribera,[a] Freek Kapteijn,[a] Eugenio Coronado[b] and Carlos J. Gómez-García*[b]

[a]*Industrial Catalysis, DelftChemTech, Delft University of Technology, Julianalaan 136, 2628BL, Delft, The Netherlands*
[b]*Instituto de Ciencia Molecular, Universidad de Valencia, Dr. Moliner 50, 46100 Burjasot, Valencia, Spain. E-mail: carlos.gomez@uv.es*

Received 13th November 2001, Accepted 23rd May 2002
First published as an Advance Article on the web 1st July 2002

The magnetic behaviour of Co–Al, Ni–Al, and Mg–Al hydrotalcites (HTlc) with a M^{2+}/Al^{3+} molar ratio of 3 and carbonates in the interlayer, as well as the mixed oxides obtained after calcination at 823 K for 5 h, has been investigated by DC and AC magnetic susceptibility measurements and isothermal magnetisation. The samples were also characterised by ICP-OES and XRD. The magnetic measurements show that Co–Al and Ni–Al HTlcs behave as ferromagnets, with ordering temperatures of approximately 6–7 K in both cases, and displaying hysteresis loops at 2 K with coercive fields of 4.2 and 5.5 mT, respectively, whereas the Mg–Al-HTlc shows the expected diamagnetic behaviour. A solid solution of cobalt spinels was the decomposition product of Co–Al-HTlc. NiO and MgO were the only crystalline phases identified in the decomposition products of Ni–Al- and Mg–Al-HTlcs, respectively. The magnetic measurements of the decomposition products confirm these data.

1 Introduction

Synthetic hydrotalcite-like compounds (HTlcs), also known as anionic clays, layered double hydroxides (LDHs), or Feitknecht's compounds, have been the subject of many studies: syntheses, preparations, and structural studies, as well as applications as sorbents, anion exchangers, catalyst supports, and catalyst precursors have been reported.[1,2] Hydrotalcites are hydrated hydroxycarbonates of random lamellar structure with the general formula $[M^{2+}_{(1-x)}M^{3+}_{x}(OH)_2][A^{m-}]_{x/m}\cdot nH_2O$, and can be visualised as brucite-type octahedral layers in which M^{3+} cations partially substitute for M^{2+} cations. The positive charge resulting from this substitution is balanced by anions (often carbonate) arranged in layers with water molecules alternating with the octahedral sheets (Fig. 1).[3,4]

From the magnetic point of view, brucite-type hydroxides of general formula $M^{2+}_{n}(OH)_m(A)_p$ (A is generally a carboxylate or dicarboxylate anion) have attracted much interest, mainly in the last five years, as these layered materials present ferro-, ferri-, antiferro-, or unusual metamagnetic behaviours,[5–14] with ordering temperatures as high as 60 K, when M^{2+} is a divalent transition ion like Co^{2+}, Ni^{2+}, or Cu^{2+}. These layered hydroxides present hysteresis cycles with coercive fields above 5 T, the highest coercive fields reported to date in any material.[15–21] From the structural point of view, these hydroxides can be related to two main structural types: (i) the brucite-type layer of edge-sharing $[MO_6]$ octahedra, where the X anions are located between the brucite-type layers replacing some of the OH^- groups and (ii) the triple-deck layer structure of $M_5(OH)_8(H_2O)_2(NO_3)_2$, formed by edge-sharing $[MO_6]$ octahedra in an hexagonal lattice and corner-sharing $[MO_4]$ tetrahedra located above and below the hexagonal holes of the octahedral layer.[22,23] Many efforts have been devoted in recent years to studying the role of the intercalated anion (charge, length, bridging mode, presence of π-electrons, ...) on the magnetic properties of these materials.[5–21] Thus, small NO_3^- anions and many different mono and dicarboxylate anions with benzene rings or with alkyl chains containing from 2 to 16 carbon atoms have been used to prepare these layered hydroxides. It should be noted that in these compounds, the anions replace some of the OH^- groups of the brucite-type layer, thus connecting the hydroxide layers through covalent bonds.

Although structurally related, hydrotalcites (HTlcs) present an important difference with these layered hydroxides: the hydroxide layers are not covalently connected through the anions (CO_3^{2-} in this case) as these counterions needed for electroneutrality just occupy the interlayer space without replacing any OH^- group. Very few magnetic studies have been performed to date with magnetic HTlcs or their thermal decomposition products.[24,25] In these few cases, the magnetic characterisation aimed to reveal the co-ordination environment and the oxidation state of the metallic ions (mainly cobalt). AC susceptibility measurements have also been performed on one thermally decomposed Co–Al–Mg hydrotalcite-like double

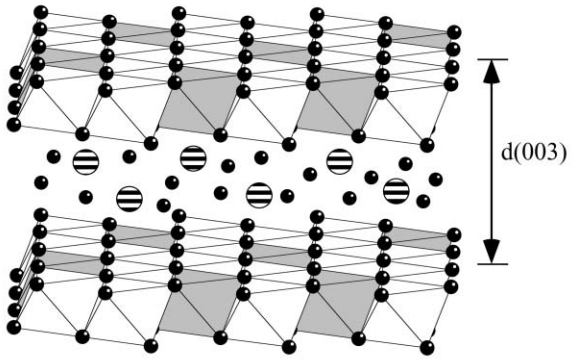

Fig. 1 Structure of HTlcs, showing the brucite-type layers with the M^{2+} and M^{3+} cations (grey and white octahedra, respectively) and the interlayer space with the CO_3^{2-} anions (stripes) and the H_2O molecules (black).

†Present address: Norsk Hydro, Research Centre, P.O. Box 2560, N-3907, Porsgrunn, Norway. E-mail: javier.perez.ramirez@hydro.com; Fax: +47 35 92 4738.

 DOI: 10.1039/b110314h

hydroxide to demonstrate the presence of small metallic cobalt particles.[26] Nevertheless, as far as we know, the magnetic properties of as-synthesised Co–Al or Ni–Al hydrotalcites have not been published to date.

In this work, we report the magnetic properties (AC and DC modes) of Co–Al, Ni–Al, and Mg–Al hydrotalcites with a M^{2+}/Al molar ratio of 3 and with carbonates in the interlayer, that can be formulated as $M^{2+}{}_6Al_2(OH)_{16}(CO_3)\cdot 4H_2O$ (M = Co, Ni, or Mg), as well as the corresponding oxides obtained after calcination at 823 K for 5 h. These samples were also characterised by ICP-OES and X-ray diffraction.

2 Experimental

2.1 Material preparation

Co–Al, Mg–Al, and Ni–Al hydrotalcites (HTlcs) were prepared by co-precipitation at constant pH and temperature at low supersaturating conditions, as previously described.[27] A flow (2 L h^{-1}) of an aqueous solution of the respective divalent metal nitrates [$Co(NO_3)_2\cdot 6H_2O$, $Ni(NO_3)_2\cdot 6H_2O$, and $Mg(NO_3)_2\cdot 6H_2O$, all >99.0% from Merck], and aluminium nitrate [$Al(NO_3)_3\cdot 9H_2O$, >99.0% from Fluka] with a total cation concentration of 1.5 M, was mixed slowly at 295 K in the required molar ratios under vigorous agitation with an alkaline solution of Na_2CO_3–NaOH. The nominal M^{2+}/Al molar ratio was 3 in all the preparations. The carbonate concentration was adjusted to obtain a CO_3^{2-}/Al^{3+} molar ratio of 2. The pH of the precipitates was kept at 9.5 by adjusting the flow rate of the alkaline solution. After addition of the reactants, the slurry was aged at 338 K for 18 h under mild stirring. A reflux unit was mounted on top of the vessel to prevent water evaporation. Finally, the material was cooled to room temperature, filtered, washed with a large amount of warm (303 K) deionised water, and dried at 363 K for 12 h. Thermal decomposition of the as-synthesised samples was carried out in static air at 823 K for 5 h, yielding the corresponding mixed oxides (denoted as *ex*-M–Al-HTlcs).

2.2 Material characterisation

The chemical composition of the as-synthesised hydrotalcite-like materials was determined by inductively coupled plasma-optical emission spectroscopy (ICP-OES) [Perkin-Elmer Plasma 40 (Si) and Optima 3000DV (axial)].

X-Ray diffraction (XRD) patterns of the as-synthesised materials and the products of calcination at 823 K for 5 h were measured using a Bruker AXS diffractometer with Bragg–Brentano geometry and Cu-Kα radiation (λ = 0.1541 nm). Data were collected in the 2θ range 5–75°, with a step size of $2\theta = 0.1°$ and a counting time of 8 s. Determination of the cell parameters of the hydrotalcite (*a* and *c*) and the decomposed oxide (*a*) samples was described in detail previously,[28] and is briefly summarised in the footnote of Table 1. The observed interplanar *d* spacings were corrected using Si as an external standard (JCPDS 27-1402).

DC magnetic measurements were performed on polycrystalline samples with a Quantum Design MPMS-XL-5 SQUID magnetometer in the temperature range 2–300 K, with an applied DC field of 100 mT. The zero field cooling measurements were performed following the standard sequence: (1) cooling the sample to 2 K in zero field (<0.005 mT), (2) warming the sample from 2 to 10 K in a field of 0.5 mT (ZFC), (3) cooling the sample from 10 to 2 K in a field of 0.5 mT (FC) and (4) warming the sample from 2 to 10 K with a zero field to measure the remnant magnetisation (RM). The isothermal magnetisations were carried out at 2 K with DC fields in the range −5 to 5 T. AC magnetic measurements were performed with an oscillating field of 0.395 mT at ten different frequencies in the range 0.1–997 Hz (0.1, 1, 5, 10, 60, 110, 190, 332, 721, and 997 Hz). The susceptibility data for the diamagnetic samples were corrected for the sample holder, previously measured in the same conditions, and for the diamagnetic contributions of the compounds as deduced by using Pascal's constant tables.

3 Results and discussion

3.1 Chemical composition

Elemental chemical analysis data indicate that the M^{2+}/Al molar ratio in the as-synthesised samples (between 2.8 and 3.0) is close to the value in the parent solutions (M^{2+}/Al = 3). This indicates that the precipitation step was carried out effectively.

3.2 X-Ray diffraction

Fig. 2 shows the XRD patterns of the as-synthesised materials. These patterns reveal that the hydrotalcite structure (JCPDS 22-700) is the only crystalline phase, exhibiting sharp and

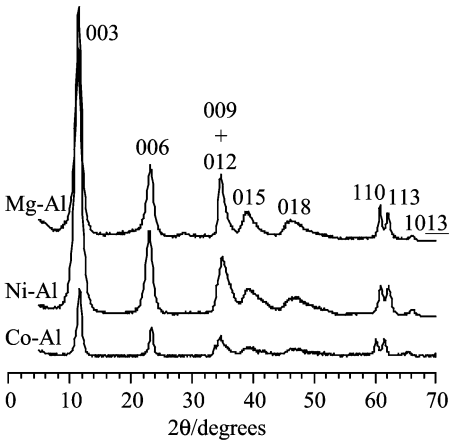

Fig. 2 X-Ray diffraction patterns of the as-synthesised Co–Al-, Ni–Al-, and Mg–Al-HTlcs.

Table 1 Data on the materials used in this study

			As-synthesised materials				
	Atomic molar ratio			Cell parameters/nm		Decomposed materials[a]	
Sample	In solution	In solid	Phases[b]	a[c]	c[d]	Phases[b]	Cell parameter a[e]/nm
Co–Al-HTlc	3 : 1	2.9 : 1	HT[f]	0.3076	2.279	Co-spinel	0.8075
Ni–Al-HTlc	3 : 1	2.8 : 1	HT	0.3035	2.253	NiO	0.4145
Mg–Al-HTlc	3 : 1	2.9 : 1	HT	0.3054	2.281	MgO	0.4203

[a]After thermal treatment of the as-synthesised hydrotalcites in air at 823 K for 5 h. [b]Crystalline, as determined from XRD. [c]From the (110) reflection of the XRD patterns (see text), corrected using Si [d(400) = 0.13579 nm, JCPDS 27-1402]. [d]From the averaged (003) and (006) reflections of the XRD patterns, corrected using Si [d(111) = 0.31379 nm, JCPDS 27-1402]. 3R polytipism for the hydrotalcite was assumed. [e]From the (440) reflection of Co-oxide and (220) reflections of Ni- and Mg-oxides of the XRD patterns, respectively, corrected using Si [d(400) = 0.13579 nm, JCPDS 27-1402]. [f]HT: hydrotalcite.

symmetric reflections for the basal (003), (006), and (009) planes, and broad and asymmetric reflections for the non-basal (012), (015), and (018) planes. The overlap of the (009) and (012) reflections results in a broad signal between $2\theta = 32$ and 38°. The (110) and (113) reflections can also be clearly distinguished. The cell parameters calculated in Table 1 are in good agreement with those reported elsewhere.[1,29]

The thermal decomposition of hydrotalcites has been described in detail elsewhere.[27,28,30] Thermal analysis coupled to mass spectrometry and *in situ* vibrational spectroscopies (infrared and Raman) provide a detailed description of the decomposition process. By calcination of Co–Al, Ni–Al, and Mg–Al hydrotalcites at 823 K for 5 h, different oxide phases are formed (Fig. 3). The cell parameters of the formed oxides are also presented in Table 1. Thermal decomposition of Co–Al-HTlc in air at 823 K for 5 h leads to the formation of a solid solution of cobalt spinels [denoted as $Co(Co,Al)_2O_4$]. Due to the similar reflection angles and intensities in XRD, it is not possible to distinguish between Co_3O_4 (JCPDS 43-1003), $CoAl_2O_4$ (JCPDS 44-160), and Co_2AlO_4 (JCPDS 38-814). Based on the molar Co/Al ratio of the as-synthesised material, a solid solution of Al^{3+} ions in Co_3O_4 is likely to be formed, as previously proposed by us.[27] In the case of the Ni–Al- and Mg–Al-HTlcs, the single oxide NiO (cubic structure, JCPDS 4-835) and MgO (cubic structure, JCPDS 45-946) are the only crystalline phases identified after thermal decomposition, respectively. $NiAl_2O_4$ and $MgAl_2O_4$ are only formed as a crystalline phase above 1073 and 1273 K, respectively.[31] The Al^{3+} ions can either be incorporated in an amorphous nickel or magnesium aluminate phase, or in a separate amorphous alumina phase (Al_2O_3).

3.3 Magnetic characterisation

3.3.1 As-synthesised hydrotalcites. The molar magnetic susceptibilities (χ_m) of the Co–Al- and Ni–Al-HTlcs show a typical Curie–Weiss behaviour at high temperatures and a sharp increase below *ca.* 6–7 K in both samples. The Curie constants obtained from the fit of the χ_m^{-1} *vs.* T plot in the high temperature region (100–300 K, with regression factors higher than 0.9999 in both samples) are 17.46(3) and 6.27(1) emu K mol^{-1}, *i.e.* values of 2.91 (4.82) and 1.04 emu K mol^{-1} (2.88 μ_B) per Co^{2+} and Ni^{2+} ion, respectively, which are very similar to those obtained for other Co^{2+} and Ni^{2+} ions in octahedral environments. The Weiss constants obtained from the same fits are −3.8(3) and 31.5(2) K for the Co–Al and Ni–Al samples, respectively. Note that the small negative value for the Co

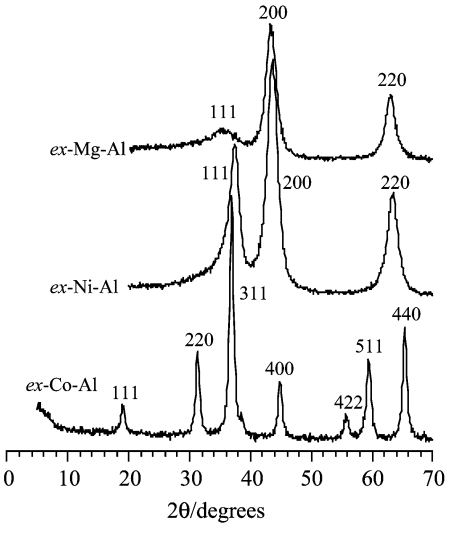

Fig. 3 X-Ray diffraction patterns of the *ex*-Co–Al-, *ex*-Ni–Al-, and *ex*-Mg–Al-HTlcs.

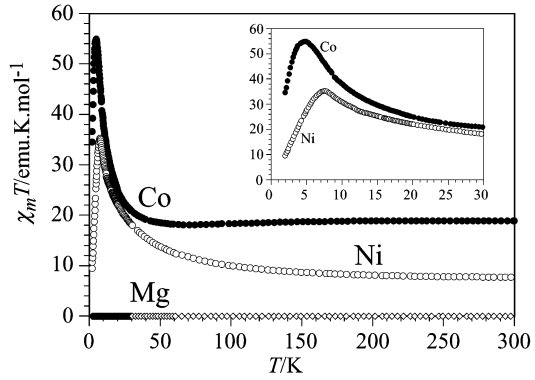

Fig. 4 Thermal variation of the $\chi_m T$ product for the Co–Al, Ni–Al and Mg–Al hydrotalcites. The low temperature region is shown in the inset.

sample is due to the presence of a spin–orbit coupling in this ion, which, in the temperature range 100–300 K, is slightly greater than the ferromagnetic Co–Co interaction. The thermal variation of the product of the molar magnetic susceptibility times the temperature ($\chi_m T$) for both samples is similar (Fig. 4), except that the Co–Al-HTlc shows a slight decrease when cooling the sample (due to the spin–orbit coupling present in Co^{2+} ions in octahedral geometry) and reaches a minimum at *ca.* 70 K. Below this temperature, $\chi_m T$ increases sharply, reaching a maximum value of 55 emu K mol^{-1} at 4.7 K, and then sharply decreases to a value of 34.5 emu K mol^{-1} at 2 K. For Ni–Al-HTlc, $\chi_m T$ increases continuously with decreasing temperature, reaching a maximum of 35 emu K mol^{-1} at 7.5 K. Below this temperature, $\chi_m T$ decreases sharply to a value of 9.5 emu K mol^{-1} at 2 K.

For Co–Al-HTlc, the magnetic behaviour suggests the presence of pairwise Co–Co ferromagnetic interactions within the brucite-like layer, which become more important than the spin–orbit coupling below 70 K. At very low temperatures, the sharp increase in the $\chi_m T$ plot, also observed in the χ_m *vs.* T plot (not shown), suggests the onset of *long-range ordering* (LRO) taking place at about 6 K. The magnetic behaviour of Ni–Al-HTlc also suggests the presence of short-range ferromagnetic Ni–Ni interactions within the brucite-like layer and the onset of LRO taking place at approximately 6 K.

Similar ferromagnetic couplings have already been observed in molecular analogues of Co^{2+} and Ni^{2+}.[32] This kind of coupling has been attributed to the orthogonality of the magnetic orbitals due to geometrical features: edge-sharing octahedra with M–O–M angles close to 90°. In the present case, the same arguments can explain the observed ferromagnetic coupling.

To confirm the presence of the LRO, zero field cooling measurements have been performed on the Co–Al and Ni–Al samples. In both cases, the results are also very similar (Fig. 5)

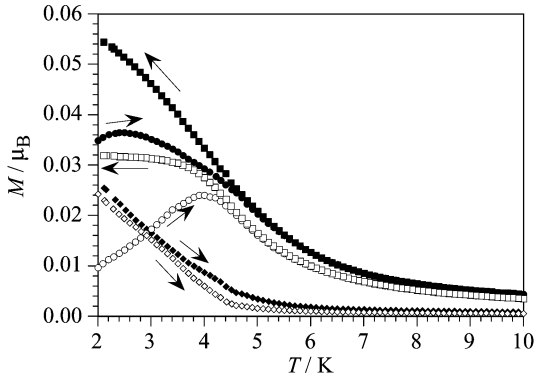

Fig. 5 ZFC (circles), FC (squares), and RM (rhombs) traces for the Co–Al (filled symbols) and Ni–Al (open symbols) hydrotalcites.

and show the typical behaviour of ferromagnetically ordered materials: (i) maxima in the ZFC scans at 2.5 (Co–Al) and 4.0 K (Ni–Al) (ii) the FC scans deviate from the ZFC scans below 5.7 (Co) and 6.0 K (Ni), and (iii) the presence of remnant magnetisation below approximately 5.5 (Co) and 5.0 K (Ni). These data confirm the presence of ferromagnetic LRO with transition temperatures of about 5.5 and 5.0 K in the Co–Al and Ni–Al samples, respectively.

Further proof of the LRO and a better determination of the ordering temperatures can be obtained from the AC susceptibility measurements (performed at different frequencies in the range 0.1–997 Hz). These measurements show very similar results for the Co–Al and Ni–Al hydrotalcites. Co–Al-HTlc shows a peak at 2.7–3.3 K in the in-phase signal (χ') (very similar to that observed in the ZFC magnetisation at 2.5 K) and a peak at 1.9–2.5 K, with a shoulder at higher temperatures (4–5 K), in the out-of-phase signal (χ''). Both features are frequency dependent, as shown in Fig. 6.

The temperature at which χ'' deviates from zero (which can be considered as the onset of the LRO), is about 6–7 K (depending on the frequency) in Co–Al-HTlc, in agreement with the DC susceptibility results (see above). A close examination of χ' and χ'' shows that the temperature of the maxima may vary from 2.7 to 3.3 K in χ' [Fig. 6(a)] and from 1.9 to 2.5 K in χ'' [Fig. 6(b)] when going from 0.1 to 997 Hz. The variation of the position of the peak in χ'' with the frequency follows an Arrhenius law: $\nu = \nu_0 \exp(-E_a/kT)$, with a frequency factor of $\nu_0 = 7.4 \times 10^{13}$ Hz and activation energy $E_a = 64$ K (Fig. 7).

The AC susceptibility measurements of Ni–Al-HTlc show similar behaviour (Fig. 8), *i.e.* peaks in the χ' and χ'' signals and a weak shoulder in the χ'' signal, which are frequency dependent. The onset of the LRO is about 6–7 K. The position of the maxima in χ' (very similar to that observed in the ZFC) and χ'' varies from 4.2 to 4.7 K [Fig. 8(a)] (4.0 K in the ZFC) and from 3.8 to 4.3 K [Fig. 8(b)], respectively, when the frequency varies from 0.1 to 997 Hz. As for the cobalt sample, the frequency dependence of the χ'' peak also follows an

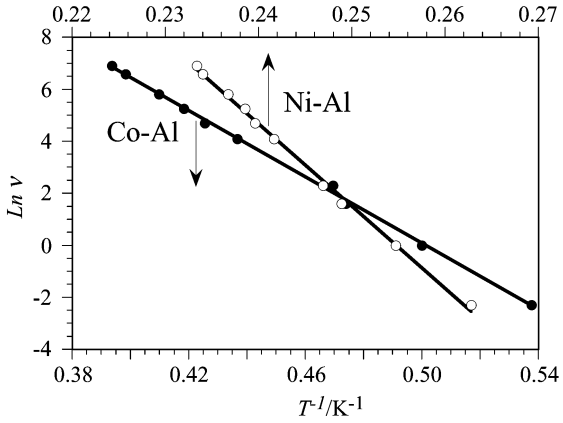

Fig. 7 Logarithm of the frequency *vs.* $1/T$ of the maximum in the out-of-phase signal (χ'') for the Co–Al- (filled circles, lower scale) and Ni–Al-HTlcs (open circles, upper scale). Solid lines are the fits to the Arrhenius law.

Arrhenius law, with $\nu_0 = 9.8 \times 10^{34}$ Hz and $E_a = 316$ K (Fig. 7).

The hysteresis cycles of both samples have been recorded at 2 K and show the presence of coercive fields of 4.2 (Co–Al) and 5.5 mT (Ni–Al) (Fig. 9). Although at 5 T the magnetisation has not completely reached saturation in both samples, the values obtained at this field (9.3 and 9.5 μ_B, for the Co–Al and Ni–Al hydrotalcites, respectively) are close to saturation and to the values expected for a parallel alignment of 6 Co^{2+} (or 6 Ni^{2+}) ions per formula unit, confirming the parallel alignment of the spins in the ordered phase.

The activated behaviours observed in both cases are typical of superparamagnets[33] and, therefore, the presence of an out-of-phase signal below the blocking temperature (6–7 K) in the AC susceptibility must be attributed to this superparamagnetic effect, which may be due to the small particle size (5–15 nm, as

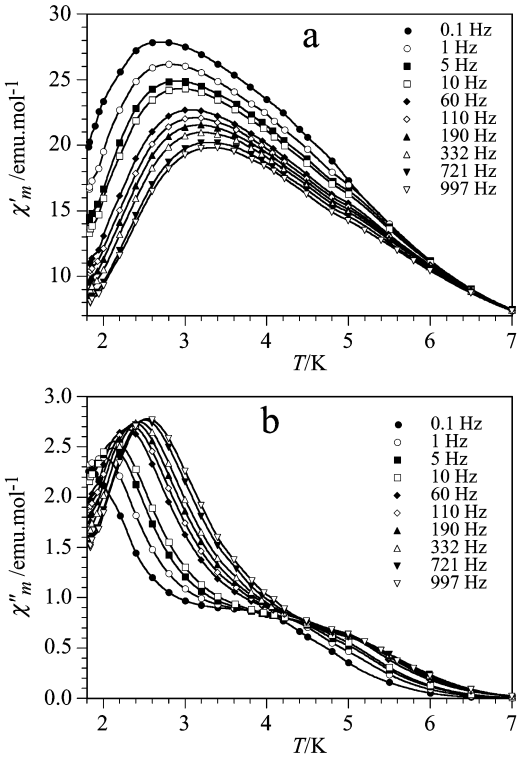

Fig. 6 Thermal dependence of (a) the in-phase signal (χ') and (b) the out-of-phase signal (χ'') of Co–Al-HTlc at different frequencies from 0.1 to 997 Hz. Solid lines are visual guides.

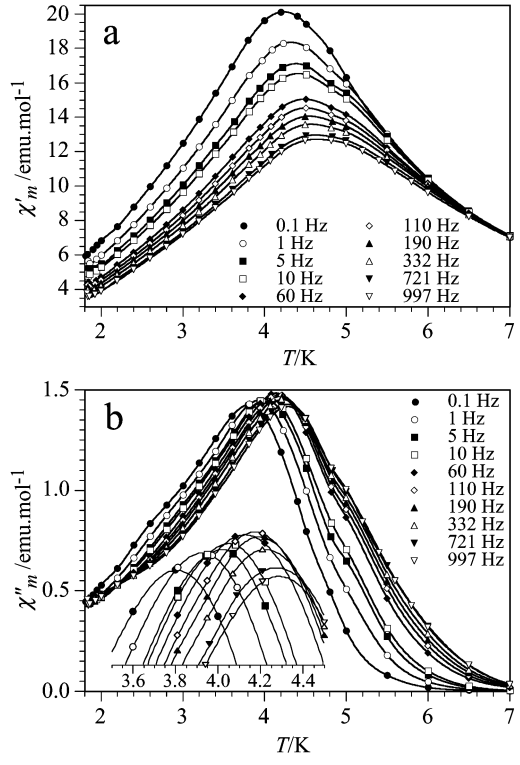

Fig. 8 Thermal dependence of (a) the in-phase signal (χ') and (b) the out-of-phase signal (χ'') of Ni–Al-HTlc at different frequencies from 0.1 to 997 Hz. Solid lines are visual guides. The inset shows the χ'' peak.

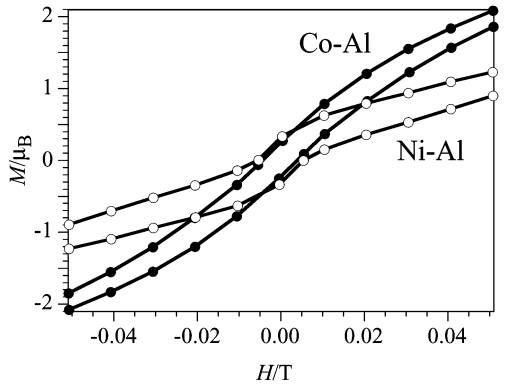

Fig. 9 Hysteresis cycles in the low field region for Co–Al- (filled circles) and Ni–Al-HTlcs (open circles) at 2 K.

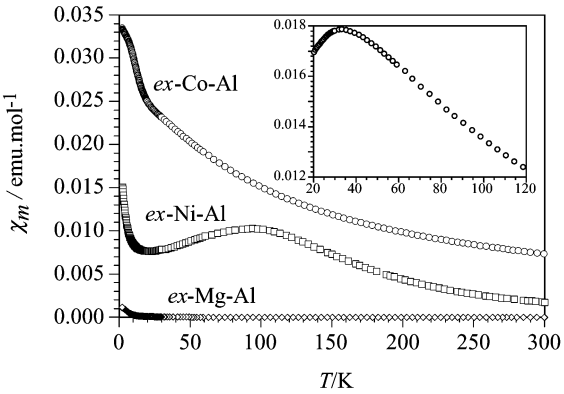

Fig. 10 Thermal variation of the molar magnetic susceptibility, χ_m, for the thermally decomposed Co–Al (circles), Ni–Al (squares), and Mg–Al (rhombs) hydrotalcites. The inset shows the plot for the cobalt sample corrected for the Curie tail.

determined from TEM, not shown) and/or to the presence of diamagnetic Al^{3+} ions, which are randomly distributed in the layer, leading to the formation of clusters of magnetic ions separated by these Al^{3+} ions.

In the Mg–Al-HTlc, both metal centres are diamagnetic and, accordingly, the magnetic susceptibility shows diamagnetic behaviour with a very small Curie constant of 4×10^{-3} emu K mol^{-1} that can be attributed to a very small amount of paramagnetic impurity coming from the Mg and/or Al precursors in the preparation.

The ferromagnetic order observed in the Co–Al and Ni–Al hydrotalcites is not surprising if we consider the structural similarity of the hydroxide layer of HTlcs and the layered hydroxides already known.[5–21] From these studies, it is to be expected that the presence or absence of covalent bonds between the hydroxide layers should not change the interlayer antiferromagnetic interaction significantly, as it is mainly dipolar in nature.[17] The LRO observed in our materials confirms this assumption. Furthermore, the relatively short interlayer distance in the Co–Al- and Ni–Al-HTlcs (determined from the c parameter as 0.759 and 0.751 nm, respectively) compared to those of the layered hydroxides (up to 4 nm) enables a stronger (antiferromagnetic) interlayer interaction and, therefore, a decrease in the ordering temperature.

The presence of a maximum and a shoulder in the χ'' signal of the hydrotalcites [see Fig. 6(a) and 8(a)] has already been observed in other layered hydroxides and was attributed to the presence of another phase.[17]

3.3.2 Thermally decomposed materials. The magnetic properties of the thermal decomposition products of the three hydrotalcites, *i.e. ex*-Co–Al, *ex*-Ni–Al, and *ex*-Mg–Al hydrotalcites are displayed in Fig. 10. As expected, the magnetic properties of the decomposition products are very different to those of the hydrotalcite precursors, except in *ex*-Mg–Al-HTlc, where the MgO obtained is also diamagnetic (as is the corresponding hydrotalcite) and thus presents a very low Curie constant of 1.5×10^{-3} emu K mol^{-1} that can also be attributed to a very small amount of paramagnetic impurity coming from the Mg and/or Al precursors. The thermal variation of the molar susceptibility, χ_m, in *ex*-Co–Al-HTlc presents a maximum at *ca.* 35 K that appears as a shoulder due to the presence of a Curie tail of around 0.16 emu K mol^{-1} at low temperatures (Fig. 10). If this Curie tail is subtracted, a maximum at *ca.* 33 K is observed (inset in Fig. 10). Nevertheless, the exact temperature of the maximum largely depends on the value of the Curie tail subtracted. This result indicates that the main phase in *ex*-Co–Al-HTlc is the spinel Co_3O_4 (which has a Néel temperature of 33 K)[34,35] rather than the possible $CoAl_2O_4$ and Co_2AlO_4 phases, whose Néel temperatures are lower and decrease with increasing the Al content.[36] This result is in agreement with the XRD data and the Co/Al molar ratio (see Fig. 3 and Table 1). Nevertheless, the presence of the Curie tail at low temperatures and the room temperature value of $\chi_m T$ (4.2 μ_B, compared to *ca.* 4.0 μ_B, which is the value expected for a Co^{2+} ion in a tetrahedral environment) suggest that a small amount of $CoAl_2O_4$ or Co_2AlO_4 may also be present in *ex*-Co–Al-HTlc. Note that the two Co^{3+} ions in the octahedral positions of the spinel are diamagnetic.[37,38]

In *ex*-Ni–Al-HTlc, the maximum in the χ_m *vs.* T plot appears at *ca.* 95 K, indicating the presence of strong antiferromagnetic Ni–Ni interactions, as has been observed in the NiO oxide.[39,40]

4 Conclusions

The magnetic properties (in AC and DC modes) of Co–Al, Ni–Al and Mg–Al hydrotalcites and their thermal decomposition products have been presented for the first time. Hydrotalcite is the only crystalline phase in the as-synthesised materials, as concluded from the XRD patterns. The DC magnetic measurements have shown that the Co–Al and Ni–Al hydrotalcites present ferromagnetic pairwise M–M interactions with ferromagnetic ordering at approximately 6–7 K in both samples. These LROs have been confirmed with hysteresis measurements, which show coercive fields of 4.2 and 5.5 mT, in the Co–Al- and Ni–Al-HTlcs, respectively. AC susceptibility measurements have showed a weak frequency dependence that may be attributed to the small particle size (5–15 nm) and/or to the presence of randomly distributed Al^{3+} ions. The magnetic properties of the oxide products are consistent with the crystalline phases identified in the XRD patterns.

Acknowledgement

This research was financially supported by the Spanish Ministerio de Ciencia y Tecnología (MAT98-0880 and FEDER project 1FD97-1765) and by the Council for Chemical Science of the Netherlands Organisation of Scientific Research (CW-NWO).

References

1 F. Cavani, F. Trifirò and A. Vaccari, *Catal. Today*, 1991, **11**, 173 and references therein.
2 A. Vaccari, *Appl. Clay Sci.*, 1999, **14**, 161 and references therein.
3 H. W. F. Taylor, *Miner. Mag.*, 1973, **39**, 377.
4 R. Allmann, *Acta Crystallogr., Sect. B*, 1968, **24**, 972.
5 M. Drillon, C. Hornick, V. Laget, F. M. Romero, S. Rouba, G. Ulrich and R. Ziessel, *Mol. Cryst. Liq. Cryst.*, 1995, **273**, 125.
6 V. Laget, S. Rouba, P. Rabu, C. Hornick and M. Drillon, *J. Magn. Magn. Mater.*, 1996, **154**, L7.

7 V. Laget, P. Rabu, C. Hornick, F. M. Romero, R. Ziessel, P. Turek and M. Drillon, *Mol. Cryst. Liq. Cryst.*, 1997, **305**, 291.
8 C. Livage, C. Egger, M. Nogues and G. Ferey, *J. Mater. Chem.*, 1998, **8**, 2743.
9 M. Kurmoo, P. Day, A. Derory, C. Estournes, R. Poinsot, M. J. Stead and C. J. Kepert, *J. Solid State Chem.*, 1999, **145**, 452.
10 T. Jestadt, M. Kurmoo, S. J. Blundell, B. W. Lovett, F. L. Pratt and W. Hayes, *Synth. Met.*, 1999, **103**, 2325.
11 C. Livage, C. Egger and G. Ferey, *Chem. Mater.*, 1999, **11**, 1546.
12 M. Kurmoo, *Chem. Mater.*, 1999, **11**, 3370.
13 C. Hornick, P. Rabu and M. Drillon, *Polyhedron*, 2000, **19**, 259.
14 K. Awaga, E. Coronado and M. Drillon, *MRS Bull.*, 2000, **25**, 52.
15 M. Kurmoo, *Philos. Trans. R. Soc. London, Ser. A*, 1999, **357**, 3041.
16 Z. L. Huang, M. Drillon, N. Masciocchi, A. Sironi, J. T. Zhao, P. Rabu and P. Panissod, *Chem. Mater.*, 2000, **12**, 2805.
17 M. Kurmoo, *Mol. Cryst. Liq. Cryst.*, 2000, **341**, 395.
18 P. Rabu, J. M. Rueff, Z. L. Huang, S. Angelov, J. Souletie and M. Drillon, *Polyhedron*, 2001, **20**, 1677.
19 B. W. Lovett, S. J. Blundell, H. Kumagai and M. Kurmoo, *Synth. Met.*, 2001, **121**, 1814.
20 P. Rabu, Z. L. Huang, C. Hornick and M. Drillon, *Synth. Met.*, 2001, **122**, 509.
21 M. Kurmoo, H. Kumagai, M. A. Green, B. W. Lovett, S. J. Blundell, A. Ardavan and J. Singleton, *J. Solid State Chem.*, 2001, **159**, 343.
22 R. Allmann, *Z. Kristallogr.*, 1968, **126**, 417.
23 W. Stählin and H. R. Oswald, *Acta Crystallogr., Sect. B*, 1970, **26**, 860.
24 P. Porta, S. Morpurgo and I. Pettiti, *J. Solid State Chem.*, 1996, **121**, 372.
25 S. Morpurgo, M. LoJacono and P. Porta, *J. Solid State Chem.*, 1996, **122**, 324.
26 A. E. Palomares, J. M. López-Nieto, F. J. Lázaro, A. López and A. Corma, *Appl. Catal., B*, 1999, **20**, 257.
27 J. Pérez-Ramírez, G. Mul, F. Kapteijn and J. A. Moulijn, *J. Mater. Chem.*, 2001, **11**, 821.
28 J. Pérez-Ramírez, G. Mul and J. A. Moulijn, *Vib. Spectroscop.*, 2001, **27**, 75.
29 J. T. Kloprogge and R. L. Frost, *Appl. Catal., A*, 1999, **184**, 2529.
30 J. Pérez-Ramírez, G. Mul, F. Kapteijn and J. A. Moulijn, *J. Mater. Chem.*, 2001, **11**, 2529.
31 T. Sato, H. Fujita, T. Endo, M. Shimada and A. Tsunashima, *React. Solids*, 1988, **5**, 219.
32 E. Coronado and C. J. Gómez-García, *Comments Inorg. Chem.*, 1995, **17**, 255.
33 J. A. Mydosh, *Spin Glasses: an Experimental Introduction*, Taylor and Francis, London, 1993.
34 W. L. Roth, *J. Phys. Chem. Solids*, 1964, **25**, 1.
35 W. Kundig, M. Kobelt, H. Appel, G. Constabaris and R. H. Lindequist, *J. Phys. Chem. Solids*, 1969, **30**, 819.
36 O. H. Hansteen, H. Fjellvag and B. C. Hauback, *Acta Chem. Scand.*, 1998, **52**, 1285.
37 A. B. P. Lever, *Inorganic Spectroscopy*, Elsevier, The Netherlands, 1968.
38 N. Kita, N. Shibuichi and S. Sasaki, *J. Synchrotron Radiat.*, 2001, **8**, 446.
39 C. de Graaf, F. Illas, R. Broer and W. C. Nieuwpoort, *J. Chem. Phys.*, 1997, **106**, 3287.
40 D. Rodic, V. Spasojevic, V. Kusigerski, R. Tellgren and H. Rundlof, *Phys. Status Solidi B*, 2000, **218**, 527.